

NONLINEAR DYNAMICS OF AN OSCILLATOR WITH A SHAPE MEMORY ALLOY DISCONTINUOUS SUPPORT

Bruno Cardozo dos Santos, *bcsantos@click21.com.br*

Marcelo Amorim Savi, *savi@mecanica.ufrj.br*

Universidade Federal do Rio de Janeiro

COPPE – Department of Mechanical Engineering

21.941.972 – Rio de Janeiro – RJ, Brazil, P.O. Box 68.503

Abstract. *In the last years, there is an increasing interest in nonsmooth system dynamics motivated by different applications including rotor dynamics, oil drilling and machining. Besides, shape memory alloys (SMAs) have been used in various applications exploring their high dissipation capacity related to their hysteretic behavior. This contribution investigates the nonlinear dynamics of shape memory alloy nonsmooth systems considering a linear oscillator with a discontinuous support built with an SMA element. A constitutive model developed by Paiva et al. (2005) is employed to describe the thermomechanical behavior of the SMA element. Numerical investigations show results where the SMA discontinuous support can dramatically change the system dynamics when compared to those associated with a linear elastic support. A parametric study is of concern showing the system behavior for different system characteristics, forcing excitation and also gaps. These results show that smart materials can be employed in different kind of mechanical systems exploring some of the remarkable properties of these alloys.*

Keywords: *Shape memory alloys, nonlinear dynamics, chaos, nonsmooth systems, contact.*

1. INTRODUCTION

Smart materials are being used in different fields of human knowledge. Shape memory alloys (SMAs) are included in the class of the smart materials and, among other characteristics, are easy to manufacture, relatively lightweight, and able of producing high forces or displacements with low power consumption. There are many applications related to SMA devices including fasteners, seals, connectors and clamps (van Humbeeck, 1999). Self-actuating fasteners, thermally actuator switches and several bioengineering devices are other important examples of SMA applications (Machado & Savi, 2002, 2003; Duerig *et al.*, 1999; Lagoudas *et al.*, 1999). Besides, the high dissipation capacity of these alloys has been employed in order to introduce a smart dissipation in system dynamics.

On the other hand, nonsmooth systems appear in many kinds of engineering systems and also in everyday life (Hinrichs *et al.*, 1998). Examples may be mentioned by the stick-slip oscillations of a violin string or grating brakes. Moreover, it is related to some related phenomena as chatter and squeal that cause serious problems in many industrial applications. Nonsmooth nonlinearity is usually associated with either the friction phenomenon or the discontinuous characteristics as intermittent contacts of some system components. Nonsmooth systems have been analyzed in order to understand various engineering problems: Oil drilling (Wiercigroch *et al.*, 2005; Franca & Weber, 2004; Pavlovskaja *et al.*, 2001), rotor dynamics (Karpenko *et al.*, 2003) and machining (Warminski *et al.*, 2003) are some interesting examples.

The objective of this research effort is to investigate the use of SMA in nonsmooth systems exploring its high dissipation capacity. This is done considering a single degree of freedom oscillator with discontinuous support. This device is previously addressed in Savi *et al.* (2007) and Divenyi *et al.* (2006) where an elastic support is treated by numerical and experimental approaches. In this contribution, the elastic discontinuous support is replaced by an SMA element and it is investigated its influence in the system dynamics. Comparisons between the system dynamics with a linear elastic and an SMA support are of concern, identifying the main aspects related to the SMA behavior.

2. CONSTITUTIVE MODEL

There are different ways to describe the thermomechanical behavior of SMAs. Here, a constitutive model that is built upon the Fremond's model and previously presented in different references (Savi *et al.*, 2002b, Baêta-Neves *et al.*, 2004, Paiva *et al.*, 2005) is employed. This model considers different material properties and four macroscopic phases for the description of the SMA behavior. The tension-compression asymmetry, the plastic strain and the plastic-phase transformation coupling are incorporated in the original model. Nevertheless, for the sake of simplicity, these characteristics are not considered in this article.

Therefore, besides strain (ε) and temperature (T), the model considers four more state variables associated with the volumetric fraction of each phase: β_1 is associated with tensile detwinned martensite, β_2 is related to compressive detwinned martensite, β_3 represents austenite and β_4 corresponds to twinned martensite. A free energy potential is proposed concerning each isolated phase. After this definition, a free energy of the mixture can be written weighting

each energy function with its volumetric fraction. With this assumption, it is possible to obtain a complete set of constitutive equations that describes the thermomechanical behavior of SMAs as presented below:

$$\sigma = E [\varepsilon + \alpha_h (\beta_2 - \beta_1)] + \alpha (\beta_2 - \beta_1) - \Omega (T - T_0) \quad (1)$$

$$\dot{\beta}_1 = \frac{1}{\eta} \left\{ \alpha \varepsilon + \Lambda(T) + (2\alpha \alpha_h + E \alpha_h^2) (\beta_2 - \beta_1) + \alpha_h [E \varepsilon - \Omega (T - T_0)] - \partial_{\beta_1} J_\pi \right\} + \partial_{\dot{\beta}_1} J_\chi \quad (2)$$

$$\dot{\beta}_2 = \frac{1}{\eta} \left\{ -\alpha \varepsilon + \Lambda(T) - (2\alpha \alpha_h + E \alpha_h^2) (\beta_2 - \beta_1) - \alpha_h [E \varepsilon - \Omega (T - T_0)] - \partial_{\beta_2} J_\pi \right\} + \partial_{\dot{\beta}_2} J_\chi \quad (3)$$

$$\begin{aligned} \dot{\beta}_3 = \frac{1}{\eta} \left\{ -\frac{1}{2} (E_A - E_M) [\varepsilon + \alpha_h (\beta_2 - \beta_1)]^2 + A_3(T) + \right. \\ \left. + (\Omega_A - \Omega_M) (T - T_0) [\varepsilon + \alpha_h (\beta_2 - \beta_1)] - \partial_{\beta_3} J_\pi \right\} + \partial_{\dot{\beta}_3} J_\chi \end{aligned} \quad (4)$$

where $E = E_M + \beta_3 (E_A - E_M)$ is the elastic modulus while $\Omega = \Omega_M + \beta_3 (\Omega_A - \Omega_M)$ is related to the thermal expansion coefficient. Notice that subscript A refers to austenitic phase, while M refers to martensite. Moreover, parameters $\Lambda = \Lambda(T)$ and $A_3 = A_3(T)$ are associated with phase transformations stress levels. Parameter α_h is introduced in order to define the horizontal width of the stress-strain hysteresis loop, while α helps vertical hysteresis loop control on stress-strain diagrams.

The terms $\partial_n J_\pi$ ($n = 1, 2, 3$) are sub-differentials of the indicator function J_π with respect to β_n (Rockafellar, 1970). The indicator function $J_\pi(\beta_1, \beta_2, \beta_3)$ is related to a convex set π , which provides the internal constraints related to the phases' coexistence. With respect to evolution equations of volumetric fractions, η and η_3 represent the internal dissipation related to phase transformations. Moreover $\partial_n J_\chi$ ($n = 1, 2, 3$) are sub-differentials of the indicator function J_χ with respect to $\dot{\beta}_n$. This indicator function is associated with the convex set χ , which establishes conditions for the correct description of internal subloops due to incomplete phase transformations and also avoids phase transformations $M^+ \rightarrow M$ or $M^- \rightarrow M$.

Concerning the parameters definition, linear temperature dependent relations are adopted for Λ and A_3 as follows:

$$\Lambda = -L_0 + \frac{L}{T_M} (T - T_M) \quad A_3 = -L_0^A + \frac{L^A}{T_M} (T - T_M) \quad (5)$$

Here, T_M is the temperature below which the martensitic phase becomes stable. Besides, L_0 , L , L_0^A and L^A are parameters related to critical stress for phase transformation.

In order to contemplate different characteristics of the kinetics of phase transformation for loading and unloading processes, it is possible to consider different values to the parameter η and η_3 , which is related to internal dissipation: η^L and η_3^L during loading while η^U and η_3^U are used during unloading process. For more details about the constitutive model, see Paiva *et al.* (2005) and Savi & Paiva (2005).

3. OSCILLATOR WITH DISCONTINUOUS SUPPORT

The dynamical response of a single-degree of freedom system with an SMA discontinuous support, shown in Figure 1, is analyzed in this contribution. The oscillator is composed by a mass m connected with two linear springs with stiffness k . Dissipation process may be modeled by a linear damping with coefficient c . Moreover, the support is massless, having a linear damping with coefficient c_s and also an element that could be either linear elastic or made by SMA. The mass displacement is denoted by x , relative to the equilibrium position and the distance between the mass and the support is defined by a gap g . Therefore, the system has two possible modes, represented by a situation where the mass presents contact with the support and other situation when there is no contact. Calling f_s as the contact force between the mass and the support, these two situations may be represented as follows:

$$\begin{cases} x < g \text{ and } f_s = 0, \text{ without contact.} \\ x \geq g \text{ and } f_s = -(K + c_s \dot{x}) < 0, \text{ with contact.} \end{cases} \quad (6)$$

where $K = K(x - g)$ represents the restitution force of the support element. By assuming an SMA support, its thermomechanical behavior needs to be evaluated from a proper constitutive equation as presented in the previous section. This element may be either a spring or a bar and, in both cases, it is possible to establish a relation between the force-displacement and the stress-strain curves (Pacheco *et al.*, 2007; Savi *et al.*, 2007). In general, one assumes that $K = B \sigma$. Notice that, if σ represents the axial stress of a bar, B represents the bar cross sectional area. On the other hand, if σ is related to a shear stress, B should be a parameter evaluated from a helical spring characteristics. Moreover, it should be highlighted that the restitution force may be assumed to be linear, $K = k_s (x - g)$, representing a linear elastic element.

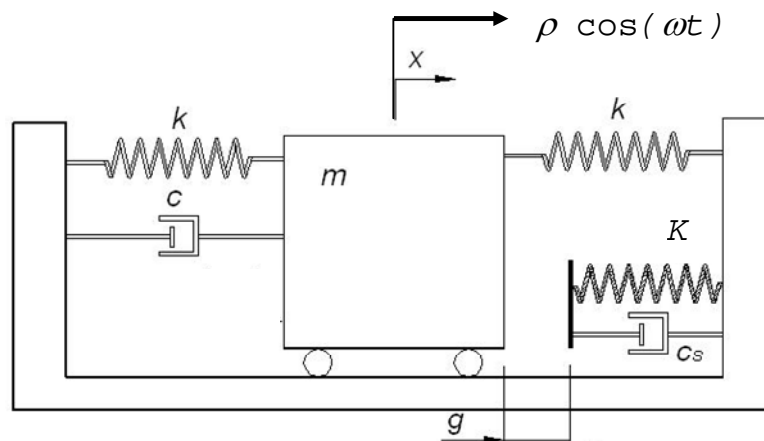


Figure 1. Nonsmooth system with discontinuous support.

According to this condition, it is written the following equations of motion:

$$\begin{cases} m\ddot{x} + 2kx + c\dot{x} = \rho \cos(\omega t), \text{ without contact.} \\ m\ddot{x} + 2kx + K + (c + c_s)\dot{x} = \rho \cos(\omega t), \text{ with contact.} \end{cases} \quad (7)$$

This system is representative of the dynamical behavior of different applications. For instance, it may be understood as a one-dimensional version of the rotor dynamics problem discussed in Karpenko *et al.* (2003) and a variation of the oil drilling problem discussed in Wiercigroch *et al.* (2005), Franca & Weber (2004) or Pavlovskaja *et al.* (2001).

A numerical procedure based on the operator split technique is employed in order to deal with the system nonlinearities. Basically, it is assumed a predictor-corrector scheme together with an iterative process. Under this assumption it is possible to use classical procedures in order to solve this problem. In this article, the fourth order Runge-Kutta method is employed to estimate the dynamical evolution of the variables. A switch model is used in order to consider the change between the situations with and without contact. Moreover, the constitutive model is solved considering the procedure developed in Savi *et al.* (2002). This process is repeated until a prescribed tolerance is assured.

4. NUMERICAL SIMULATIONS

Numerical simulations regarding the nonlinear dynamics of a single degree of freedom oscillator with discontinuous support are of concern. Two different situations are of concern: linear elastic support and SMA support. In order to allow a comparison between results predicted by both models, it is assumed the same oscillator characteristics and also an SMA support with the same austenitic elastic response than the elastic support. Under this condition, it is possible to establish the main effects related to the phase transformations in SMA response. This section considers a parametric analysis investigating the effect of different parameter variations. Basically, it is investigated the influence of dissipation, forcing parameters (frequency and amplitude) and gap.

All simulations consider the following oscillator parameters: $m = 0.838$ kg, $k = 8.47$ N/m. Moreover, the support parameters are: $k_S = 1350$ N/m (elastic support), and $B = 2.5 \times 10^{-8}$ m² (SMA support). Other parameters are varied depending on the analysis.

Table 1. SMA constitutive parameters.

E_A (GPa)	E_M (GPa)	α (MPa)	ε_R
54	42	150	0.055
L_0	L	L_0^A	L^A
0.15	4	6.3	165
Ω_A (MPa/K)	Ω_M (MPa/K)	T_M (K)	T_0 (K)
0.74	0.17	291.4	298
η^L (MPa.s)	η^U (MPa.s)	η_3^L (MPa.s)	η_3^U (MPa.s)
8	2	5	5

4.1. Dissipation Effects

The nonlinear dynamics analysis of the oscillator with discontinuous support starts considering the effect of dissipation. It is assumed $c_S = 0.6$ Ns/m, $g = -0.0045$ m and forcing parameters $\rho = 4.5$ N and $\omega = 2.3$ rad/s. In order to obtain a global understanding of the system behavior, bifurcation diagrams are presented showing the stroboscopic sample of state variables (displacement and velocity) under the slow quasi-static variation of dissipation parameter c . Elastic and SMA support system responses are plotted together in Figure 2. The elastic support system presents a complex behavior, presenting chaotic like response for low values of dissipation parameter. The more this parameter is increased, the less complex is the system response. On the other hand, the response of the system with SMA support dissipates energy enough to obtain a less complex behavior for all dissipation parameters.

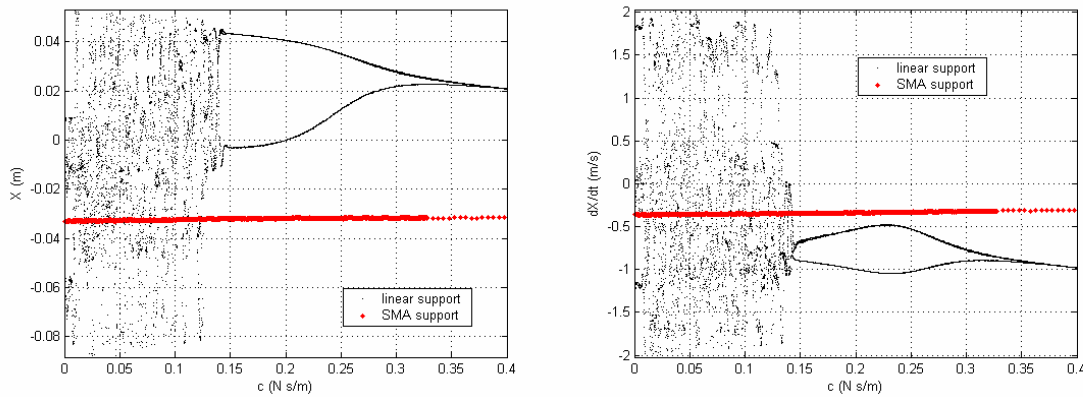


Figure 2. Bifurcation diagram varying dissipation parameter.

Different parameter values are now in focus in order to show each system response characteristics. Figure 3 shows the system response for $c = 0.05$ Nm/s, a value inside the chaotic region of the elastic support system. The elastic support system response is chaotic like, presenting a strange attractor with fractal like structure. On the other hand, the SMA support system presents a periodic response. This difference may be understood by observing the high dissipation capacity of the SMA system due to hysteresis loop. Figure 4 presents the force-displacement curve of both supports during the response. The SMA hysteresis loop dissipates an amount of energy responsible for the chaotic response of the elastic system. By observing the frequency spectrum (Figure 5) it is also noticeable that the energy is spread over a wider bandwidth in the elastic support system response.

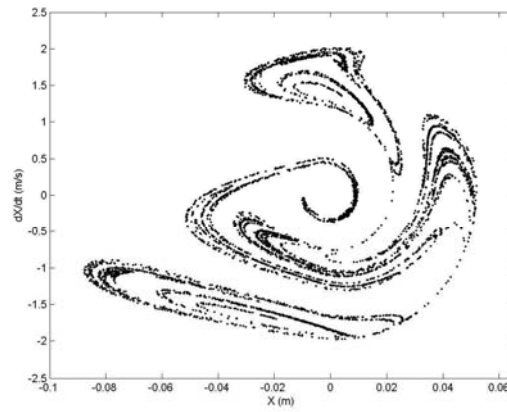
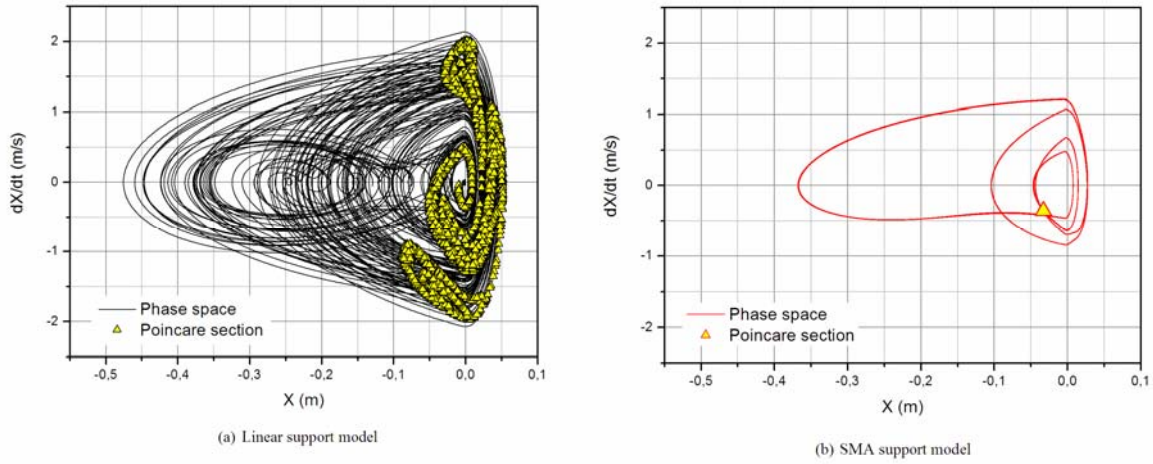


Figure 3. Systems response for $c = 0.05$ Nm/s.

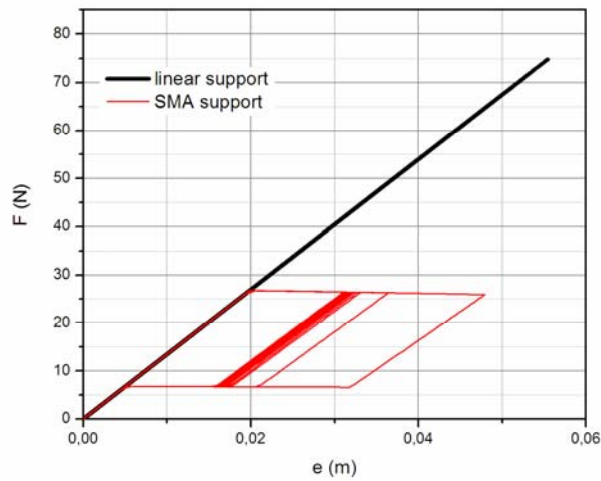


Figure 4. Force-displacement curve for $c = 0.05$ Nm/s.

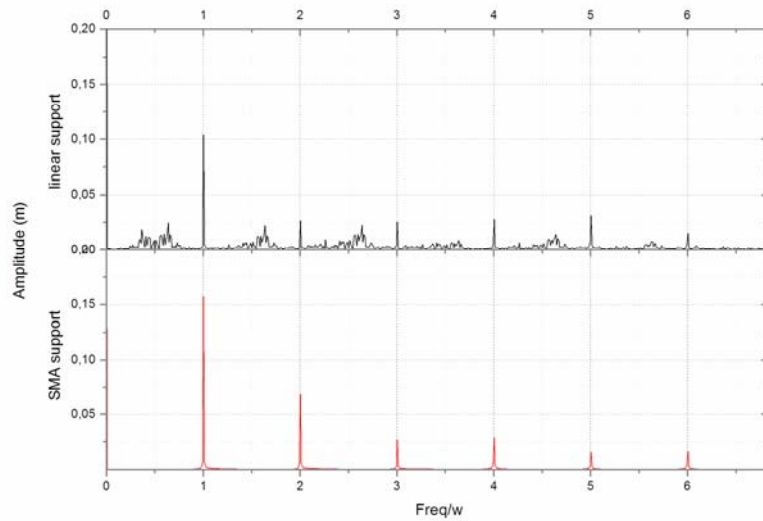


Figure 5. Frequency spectrum response for $c = 0.05$ Nm/s.

At this point, it should be highlighted that the SMA support introduces dissipation to the system dramatically changing its response. Notice that the increase in the system dissipation by changing the dissipation parameter tends to homogenize the behaviors related to elastic and SMA support.

4.2. Forcing Characteristic Effects

The forcing characteristics effects are now in focus. It is assumed $c = 0.3$ Ns/m, $c_s = 0.6$ Ns/m, $g = 0.02$ m. Bifurcation diagrams are presented showing the stroboscopic sample of state variables (displacement and velocity) under the slow quasi-static variation of forcing parameters. Forcing frequency is analyzed first assuming $\rho = 4.5$ N. Linear elastic and SMA support system responses are plotted together in Figure 6. Once again, the high dissipative behavior of SMA support tends to produce less complex behaviors when compared to those from elastic support. Figure 7 presents a sequence of Poincare sections for different frequency values showing the system evolution. The mentioned difference between elastic and SMA support responses is clear noticeable.

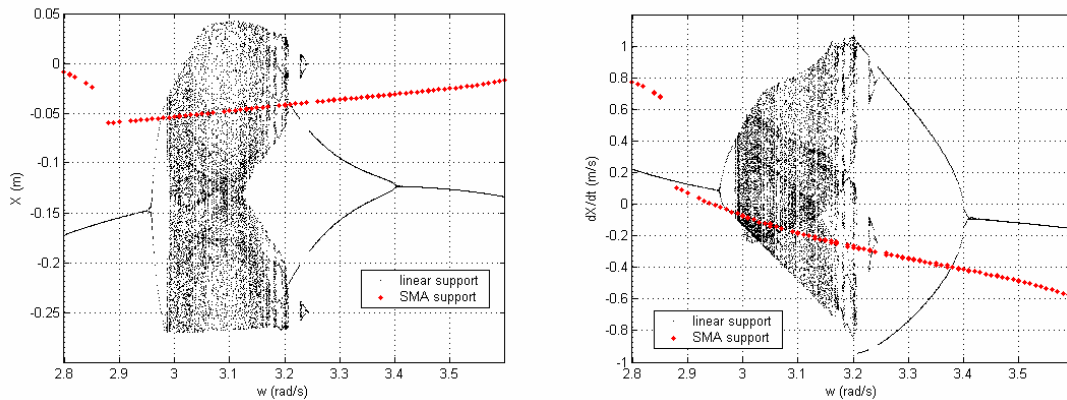


Figure 6. Bifurcation diagrams varying amplitude frequency.

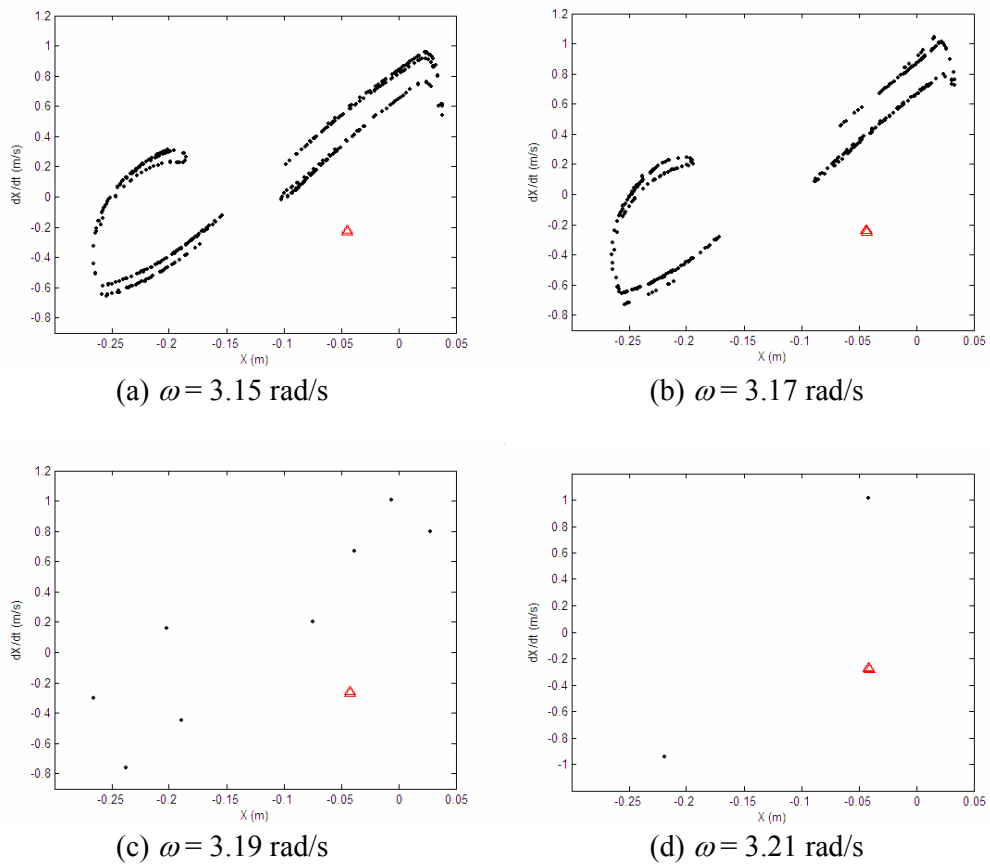


Figure 7. Sequence of Poincaré sections for different frequency values.

The same kind of behavior may be expected concerning the forcing amplitude effect. Figure 8 presents the bifurcation diagram associated with this parameter, assuming $\omega = 4.5$ rad/s. For low amplitude values, both systems present the same behavior since SMA hysteresis loop is not reached. The increase of this amplitude, however, tends to change the system responses. Figure 9 presents the response of both systems for $\rho = 2.1$ N. Notice that elastic support system response is chaotic like while the SMA support response is periodic.

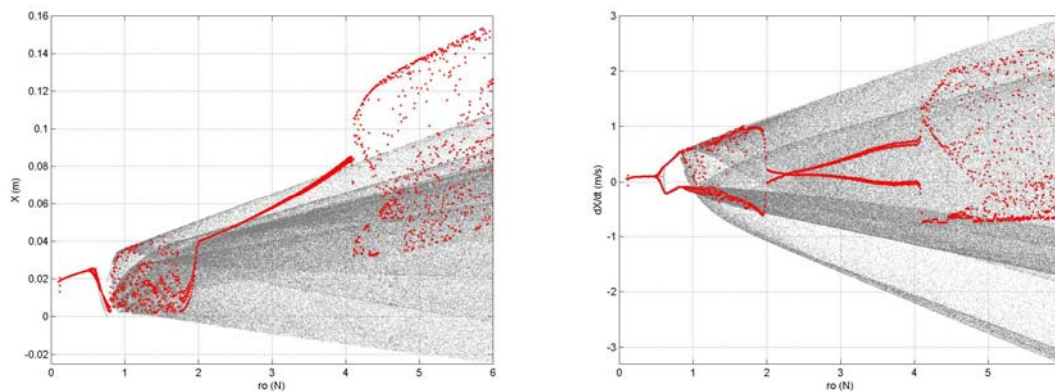


Figure 8. Bifurcation diagram varying the forcing amplitude.

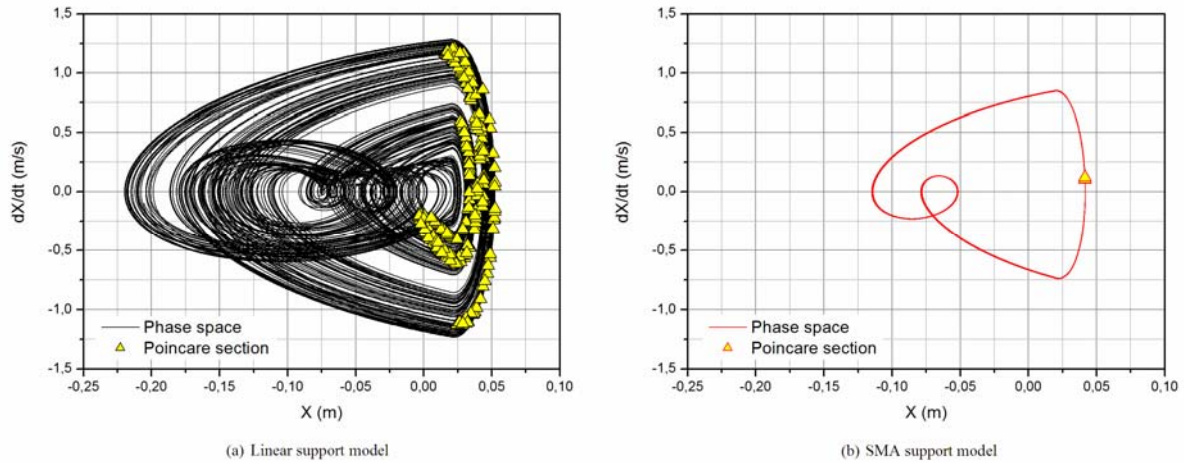


Figure 9. System response for $\rho = 2.1$ N.

4.3. Gap Effects

The parametric study now contemplates the gap influence on the nonlinear dynamics of the oscillator with discontinuous support. Now, it is assumed $c = 0.87$ Ns/m, $c_S = 0.6$ Ns/m and forcing parameters $\rho = 4.5$ N and $\omega = 2.3$ rad/s. The analysis is started by presenting the bifurcation diagrams changing the gap parameter. Elastic and SMA support system responses are plotted together in Figure 10. The elastic support system presents a complex behavior, presenting bifurcations and chaos as the gap change. Once again, the SMA system response dissipates energy enough to obtain a less complex behavior for all gap parameter.

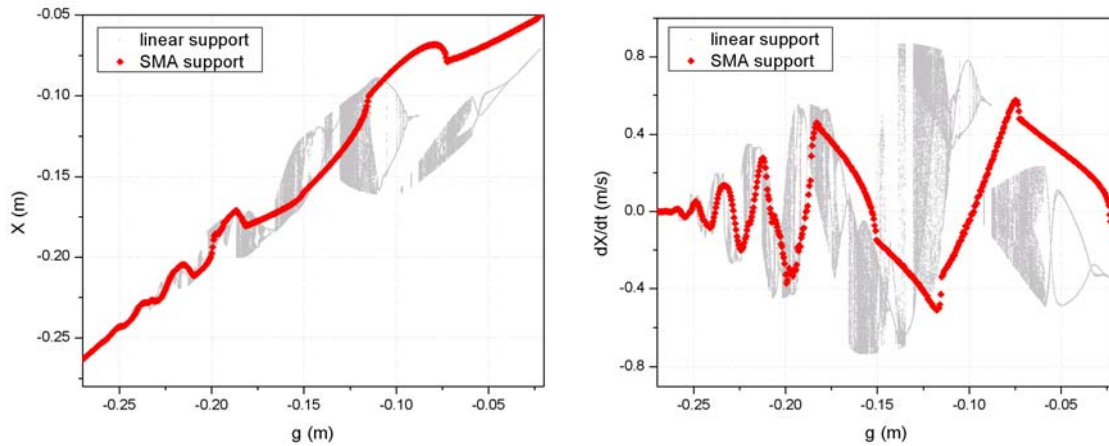


Figure 10. Bifurcation diagram varying the gap.

Different gap values are now in focus in order to compare results of both systems. At first, $g = -0.124$ m is considered (Figure 11). Under this condition, elastic support system presents a chaotic like response while SMA support system has a period-1 response. By changing the gap for $g = -0.04$ m (Figure 12), both systems have periodic responses showing that reducing the negative gaps tends to less complex behaviors.

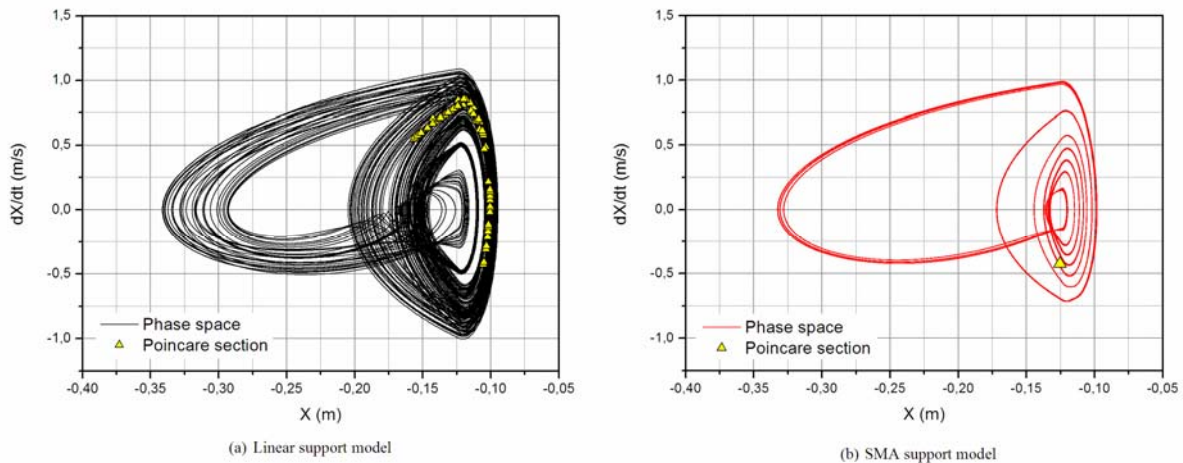


Figure 11. System response for $g = -0.124$ m.

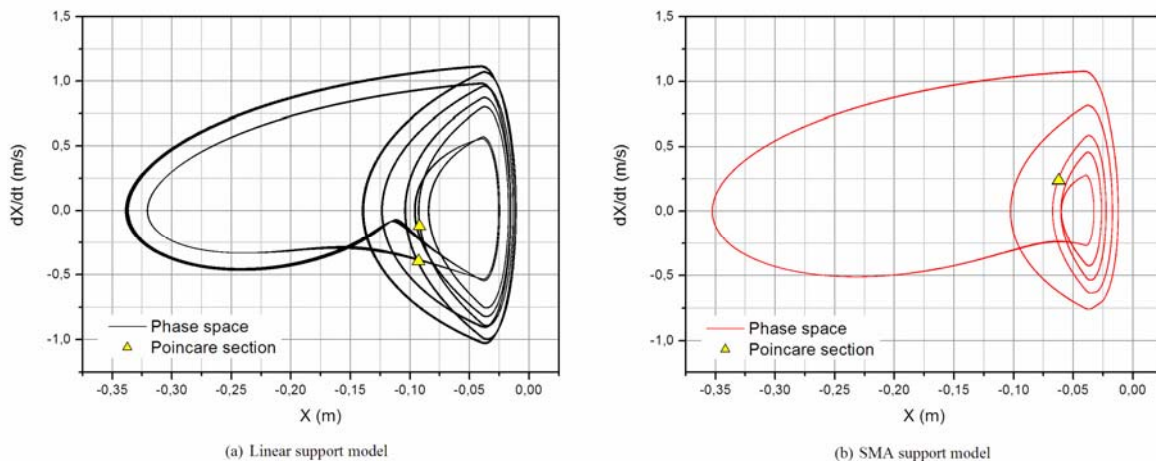


Figure 12. System response for $g = -0.04$ m.

5. CONCLUSIONS

This contribution discusses the nonlinear dynamics response of a single degree of freedom oscillator with a discontinuous SMA support. The thermomechanical behavior of the SMA is described by a constitutive model proposed by Paiva *et al.* (2005). Results of this system are compared with those obtained considering an elastic support. A parametric analysis is carried out considering the effects of system dissipation, forcing characteristics and gap. Moreover, it is shown the effect of the SMA support in order to avoid undesirable effects under resonant conditions. In general, it is possible to conclude that the high dissipation capacity of SMA due to hysteresis loop is capable to produce less complex behaviors, dramatically changing the system response. Concerning engineering applications, it should be notice that SMA support can be imagined as passive vibration control avoiding inconvenient transients during starting and stopping machines. Besides, SMA support may avoid some kinds of bifurcations, simplifying dynamical system response and allowing the energy use in a desirable frequency.

6. ACKNOWLEDGEMENTS

The authors acknowledge the support of Brazilian Research Council (CNPq).

7. REFERENCES

- Baêta-Neves, A.P., Savi, M.A. & Pacheco, P.M.C.L., 2004, "On the Fremond's constitutive model for shape memory alloys", *Mechanics Research Communications*, v.31, n.6, pp.677-688.
- Divenyi, S., Savi, M. A., Franca, L. F. P. & Weber, H. I., 2006, "Nonlinear dynamics and chaos in systems with discontinuous support", *Shock and Vibration*, v.13, n.4/5, pp.315-326.

- Duerig, T. M., Pelton, A. & Stöckel, D., 1999, "An overview of nitinol medical applications", *Materials Science and Engineering A*, v.273-275, pp.149-160.
- Franca, L.F.P. & Weber, H.I., 2004, "Experimental and numerical study of a new resonance hammer drilling model with drift", *Chaos, Solitons and Fractals*, v.21, pp.789–801.
- Hinrichs, N., Oestreich, M. & Popp, K., 1998, "On the modelling of friction oscillators", *Journal of Sound and Vibration*, v.216, n.3, 435-459.
- Karpenko, E.V., Pavlovskaja, E.E. & Wiercigroch, M., 2003, "Bifurcation analysis of a preloaded Jeffcott rotor", *Chaos, Solitons and Fractals*, v.15, pp.407–416.
- Lagoudas, D. C., Rediniotis, O. K. & Khan, M. M., 1999, "Applications of shape memory alloys to bioengineering and biomedical technology", *Proceeding of 4th International Workshop on Mathematical Methods in Scattering Theory and Biomedical Technology*, Perdika, Greece.
- Leine, R. I., 2000, "Bifurcations in discontinuous mechanical systems of Filippov-type", Ph.D. Thesis, Technische Universiteit Eindhoven.
- Machado, L. G. & Savi, M. A., 2003, "Medical applications of shape memory alloys", *Brazilian Journal of Medical and Biological Research*, v.36, n.6, pp.683-691.
- Machado, L. G. & Savi, M. A., 2002, "Odontological applications of shape memory alloys", *Revista Brasileira de Odontologia*, v.59, n.5, pp.302-306 (in portuguese).
- Pacheco, P. M. C. L., Savi, M. A. & Paiva, A., 2007, "Phenomenological modeling of shape memory alloy helical spring", *COBEM 2007 – 19th International Congress of Mechanical Engineering*.
- Pacheco, P. M. C. L. & Savi, M. A., 2000, "Modeling and simulation of a shape memory release device for aerospace applications", *Revista de Engenharia e Ciências Aplicadas*.
- Pavlovskaja, E., Wiercigroch, M. & Grebogi, C., 2001, "Modeling of an impact system with a drift", *Physical Review E*, v.64, n.5, Art. No. 056224.
- Piironen, P. T., Virgin, L. N. & Champneys, A. R., 2004, "Chaos and period-adding: Experimental and numerical verification of the grazing bifurcation", *Journal of Nonlinear Science*, v.14, pp.383–404.
- Paiva, A. & Savi, M.A., 2006, "An overview of constitutive models for shape memory alloys", *Mathematical Problems in Engineering*, v.2006, Article ID56876, pp.1-30.
- Paiva, A., Savi, M. A., Braga, A. M. B. & Pacheco, P. M. C. L., 2005, "A Constitutive Model for Shape Memory Alloys Considering Tensile-Compressive Asymmetry and Plasticity", *International Journal of Solids and Structures*, v.42, n.11-12, pp.3439-3457.
- Savi, M.A., Sa, M.A.N., Paiva, A. & Pacheco, P.M.C.L., 2007, "Tensile-Compressive Asymmetry Influence on the Shape Memory Alloy System Dynamics", *Chaos, Solitons & Fractals*.
- Savi, M.A., Divenyi, S., Franca, L.F.P. & Weber, H.I., 2007, "Numerical and experimental investigations of the nonlinear dynamics and chaos in non-smooth systems", *Journal of Sound and Vibration*, v.301, n.1-2, pp.59–73.
- Savi, M.A. & Paiva, A., 2005, "Describing internal subloops due to incomplete phase transformations in shape memory alloys", *Archive of Applied Mechanics*, v.74, n.9, pp.637-647.
- Savi, M. A., Paiva, A., Baêta-Neves, A. P. & Pacheco, P. M. C. L., 2002, "Phenomenological Modeling and Numerical Simulation of Shape Memory Alloys: A Thermo-Plastic-Phase Transformation Coupled Model", *Journal of Intelligent Material Systems and Structures*, v.13 n.5, pp. 261-273.
- van Humbeeck, J., 1999, "Non-medical Applications of Shape Memory Alloys", *Materials Science and Engineering A*, v.273-275, pp.134-148.
- Warminski, J., Litak, G., Cartmell, M.P., Khanin, R. & Wiercigroch, M., 2003, "Approximate analytical solutions for primary chatter in the non-linear metal cutting model", *Journal of Sound and Vibration*, v.259, n.4, pp.917-933.
- Wiercigroch, M., Wojewoda, J. & Krivtsov, A.M., 2005, "Dynamics of ultrasonic percussive drilling of hard rocks", *Journal of Sound and Vibration*, v.280, n.3-5, pp.739-757.

8. RESPONSIBILITY NOTICE

The author(s) is (are) the only responsible for the printed material included in this paper.